The mechanical effects of kissing bonding defects in hybrid metal-composite laminates

Drożdziel, Magda; Podolak, Piotr; Nardi, Davide; Jakubczak, Patryk

DOI
10.1016/j.compstruct.2021.114027

Publication date
2021

Document Version
Final published version

Published in
Composite Structures

Composite Structures 269 (2021) 114027

Contents lists available at ScienceDirect

Composite Structures

journal homepage: www.elsevier.com/locate/compstruct

The mechanical effects of kissing bonding defects in hybrid metal-composite laminates

Magda Droździel [a,*], Piotr Podolak [a], Davide Nardi [b], Patryk Jakubczak [a]

[a] Lublin University of Technology, Faculty of Mechanical Engineering, Department of Materials Engineering, Nadbystrzycka st. 36, 20-618 Lublin, Poland
[b] Delft University of Technology, Faculty of Aerospace Engineering, Department of Aerospace Structures and Materials, Kluyverweg 1, 2629 HS Delft, Netherlands

ARTICLE INFO

Keywords:
FML
Kissing bonds
NDT
Adhesion
Single lap
T-peel

ABSTRACT

Fibre metal laminates (FML) are hybrid materials perspective for wind-turbine, containers and marine objects, besides the aerospace industry. During the manufacturing process some faults can occur and can be hazardous for the reliability of FML structures. One of the most critical defects are kissing bonding due to their lack of detectability and strength compared to traditional delamination defect. The quantitative explanation were under consideration, such as loads effects; material properties; prediction of response; fracture analysis. The purpose of this work is the evaluation the impact of this type of defect on the part in-plane and the out-of-plane mechanical properties. It was presented that even responsive NDT methods are not able to detects the kissing bonding defect in FML components. Simultaneously, the kissing bonding impact on mechanical properties in FML is significant. In the case of FMLs with the orientation of the fibre perpendicular to the peel direction there is one failure pattern which is interlayer fracture. Whereas in the case of FMLs with the direction of the fibres longitudinal to the peel direction two failure patterns occur which is interlayer fracture and translaminar fibre crack. Depending on the kissing bonding area width the interlayer fracture in the composite can be observed until kissing bonding defect area and then transmission of the crack to the metal/composite interface through the fibres. In the case of low extension of poor adhesion area, the two parallel interlaminar cracking can be seen, one at the metal/composite interface in poor adhesion area, the second continuous in the composite layer.

1. Introduction

Fibre metal laminates (FML) are hybrid materials perspective for wind-turbine, containers and marine objects, besides the aerospace industry. The base of FMLs construction is connection of thin metal sheets with fibre-reinforced-polymer composites without adhesive films [1,2] or other adhesive interlayers since the fracture toughness of the metal/composite interface is provided by an appropriate metal surface preparation, such as anodizing and primer with a corrosion inhibitor [3,4]. FMLs are characterized by unique properties such as fatigue [5,6], corrosion [7–9] and impact resistance [10–12]. Nevertheless, delaminations at the metal/composite interface are critical and adversely affect the strength properties [13–15]. The fracture toughness of a metal/composite interface constitutes the weakest factor of FMLs [10,16]. The fracture of the metal/composite interface in FMLs can be initiated because of external load conditions, especially impact [17,18] and fatigue [19,20]. The high adhesion properties provide an effective bridging effect (increasing the fatigue resistance) and prevent the mode I fracture (increasing the local buckling tendency and post-impact compression resistance). However, manufacturing induced defects can be also extremely hazardous for the structural reliability. Abouhamzeh M. et. al. [21] presented the experimental analysis of the effect of gaps and overlaps on the mechanical properties of FMLs. The authors reported the significant reduction of tensile and interlaminar shear strengths. Croft et al. [22] concluded that, there are cases in which the reduction of mechanical properties due to manufactured defects is even 13%. Also Lan et al. [23] reported significant changes of tensile properties of FMLs with manufacturing defect such as kissing bonds.

The solution to the problem of manufactured and operational defects in FMLs is via non-destructive evaluation procedures. Until now, a lot of works have been published about ultrasonic testing methods [24–26] and others NDT [27–29] reliable for FMLs. All of them are based on simulated defects with foreign objects or true damage caused

* Corresponding author.
E-mail address: m.drozdziel@pollub.pl (M. Droździel).

https://doi.org/10.1016/j.compstruct.2021.114027
Received 15 March 2021; Revised 15 April 2021; Accepted 28 April 2021
Available online 4 May 2021

Nomenclature

FML	[−] fibre metal laminates
(0)	[−]fibre orientation along to the major axis (length of the sample)
(90)	[−]fibre orientation perpendicular to the major axis (length of the sample)
SSR	[−]signal to signal ratio
$f(x_n,y_m \notin d_a)\_S_A$	[%]the value of the signal outside the kissing bonding area
$f(x_k,y_p \in d_a)\_S_B$	[%]the value of the signal in the kissing bonding area
d_a	[mm^2] the area of defect
x_n ; y_m ; x_k ; y_p	[−]point coordinates linked with sample geometry
W	[J] the rate of total external work
γ	[J] the debonding energy per unit area of crack advance
δ	[J] the dissipative energy per unit area of crack advance
b	[mm] sample width
_x	[mm] width of kissing bonding area
v	[m/s] velocity of point of application of peel forces
P	[N] peel force
G_{Ic}	[N/mm] adhesive fracture energy in mode I
G_Ic'	[N/mm] distorted adhesive fracture energy in mode I in kissing bonding area
σ	[MPa] cleavage stress at distance d of metal - composite adhesive
σ_0	[MPa] boundary cleavage stress at d = 0
d	[mm] the distance along t-peel of adhesive
Y	[GPa] Young modulus of adhesive
E	[GPa] Young modulus of adherend
a	[mm] adhesive layer thickness
w	[mm] adhesive width
I	[mm^4] moment of inertia of the adherent cross-section
m	[N*mm] moment arm of peel force
θ	[°] peel angle
Ω	[rad] the angle between peeled arms
Ω_1	[rad] the angle between peeled arms before kissing bonding
Ω_2	[rad] the angle between peeled arms over the kissing bonding area

by e.g. impact loads. It should be noted that these classes of defects are not the only cases in which the risk of rapid degradation of mechanical properties during operation of real structures can occur. One of the most critical are zero thickness delamination type of defects, namely kissing bonding defects or zero volume bonds [30]. The kissing bonding is an area at the layer interface where the two surfaces are held together by a compressive stress with no molecular forces acting between them [31,32]. Jiao and Rose [33] defined a kissing bond as a perfect contact between two surfaces which transmits no shear stress. The kissing bonding defect can also occur in layered structures such as composites, and structures with adhesive joints. The source of the kissing bonding defect is the manufacturing process were release agents are used during the molding process of composites [34]. The problem of kissing bonding in term of NDT effectiveness, as well as the effect on the mechanical properties, were investigated a couple times. Tighe et al. [35] described the problem of the identification of kissing defects in adhesive bonds using infrared thermography. They concluded that the kissing bonding caused the bond to fail via adhesive failure and cannot be identified through material thermal contrasts. Jeenjitkaew and Guild [36] presented work where the objective was the demonstration that the strength of joints containing kissing bonds can be predicted using FEA, and that local measurement of strain around kissing bonds could form a basis for their monitoring or detection. Moreover, Jeenjitkaew and Guild [36] presented that the kissing bonding defects can make an adhesive joint strength reduction up to 35%. Markatos et al. [34] focused on the effects of manufacturing-induced and in-service related bonding quality reduction on the mode-I fracture toughness of composite bonded joints. Authors showed that conventional NDT, such as ultrasonic and X-ray inspection, are not capable to sufficiently detect the kissing bonding defects. Simultaneously, authors have shown that the release agent can reduce the fracture toughness of the bonded joints even about 70% of the nominal strength.

Kissing bonding in FMLs has not been evaluated yet. FMLs are materials with numerous interfaces with different physical properties, which is problematic for NDT methods. Also, the proper adhesion at the interfaces is critical for fatigue or post-impact properties. Moreover, the current approaches for the evaluation of kissing bonding in adhesive joints, cannot be straightly transferred to FMLs because of the different nature of metal/composite connection and share of fibres in stresses transfer. The aim and innovative aspects of this work refer to the problem of the impact of this type of defect to in-plane and out-of-plane mechanical properties. The mechanics of complex hybrid structures is the direct core of the work. The experimental and analytical approach is used to recognize fracture phenomena. The description of these aspects can be helpful in understanding the kissing bonding impact to reliability of FML and represent the beginning of better manufacturing processes design and non-destructive testing methods.

2. Materials and methods

2.1. FMLs and kissing bonding defect

FMLs based on aluminum (2024-T3) and unidirectional carbon prepreg (single layer thickness 0.05 mm, EP135, NTPT, Switzerland) were tested. Such FMLs are one of the new generations of FML, perspective for wide application in the machine and building industry. The scheme of tested laminates is presented in Table 1. Different kissing bond widths (Fig. 1) were considered to evaluate a threshold on the effect of the defects on the laminate's mechanical properties. The laminates were labelled as follows:

SLS – sample for single lap shear test
TP – sample for t-peel test
REF – reference sample without kissing bonds

Table 1
The scheme of tested laminates.

No.	FML description	Layer sequence	Fibre orientation	Kissing bonding width [mm]	Number of samples	Test
1	SLS_Ref	Al/CFRP	0°	0	3	NDT,
2	SLS_5mm	$(0)_2$/Al	0°	5	3	SLS
3	SLS_10mm		0°	10	3	
4	SLS_15mm		0°	15	3	
5	SLS_20mm		0°	20	3	
6	TP_0_Ref	Al/CFRP	0°	0	5	NDT,
7	TP_0_4mm	$(0)_2$/Al	0°	4	5	T-peel
8	TP_0_12mm		0°	12	5	
9	TP_0_20mm		0°	20	5	
10	TP_90_Ref	Al/CFRP	90°	0	5	
11	TP_90_4mm	$(90)_2$/Al	90°	4	5	
12	TP_90_12mm		90°	12	5	
13	TP_90_20mm		90°	20	5	

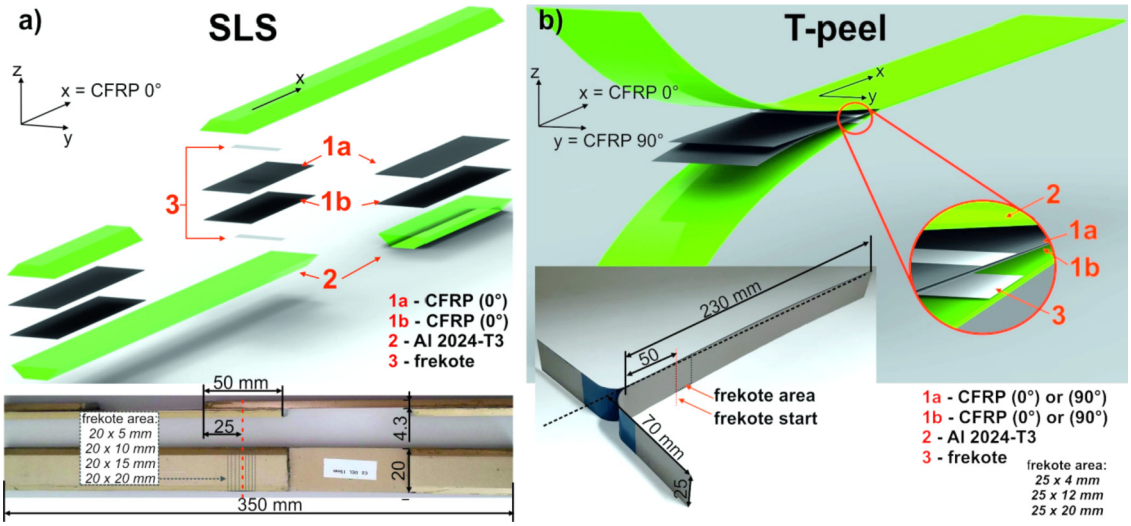

Fig. 1. The scheme of samples for SLS (a) and T-peel (b) tests.

(0) - fibres 0° – along the sample length
(90) - fibres 90° – perpendicular to sample length
_x mm – width of kissing bonding area

The lay-up sequence of the tested laminates was 0° (along the sample length) for Single Lap Shear (SLS) tests and 0° and 90° for T-peel test. The single layer of aluminum has the thickness of 4.3 mm and 0.3 mm for SLS and T-peel samples respectively. The selected fibre orientations represent two extreme mechanical responses at the metal-composite interfaces. It is connected with the stress direction, where stresses along fibre direction are transferred to the fibres while perpendicular is transferred mostly to the matrix between fibres.

The kissing bonding defect was simulated by using a release agent "frekote" (PTFE based liquid foil, Airtech Safelease #30 Mold Release, Airtech International Inc, USA), placed on the metal sheet surface by a nonwoven fabric wipe (Sontara, Scotch Brite, 3 M, USA). The frekote release agent was applied on the surface of two aluminium layers. The samples views and kissing bonding location are presented in Fig. 1.

Laminates were manufactured by using an autoclave method (Sholtz Mashinenbau, Germany) with the stages and parameters presented in Table 2.

Table 2
The scheme of FMLs flat panels and samples manufacturing.

Step no.	Name of the manufacturing stage	Stage details
1	Preparation	prepreg cutting, metal sheets cutting, quality control key parameters: not applicable
2	Kissing bonding	frekote deposition on metal sheets, air drying key parameters: step total time 12 h
3	Lamination	lamination layer by layer in clean room key parameters: not applicable
4	Vacuum bag	vacuum bag [37] key parameters: vacuum − 0.08 MPa
5	Curing process	Pressure temperature 1 - time > temperature 2 - time > cooling key parameters: pressure 0.4 MPa through the total process time 8.5 h temperature 80 °C through 2 h > 150 °C through 3 h > 30 °C heating and cooling temperature rate 1.2 °C/min.
6	Samples preparation and quality control	Abrasive cutting, macroscopic analysis of samples key parameters: not applicable

2.2. Non-destructive tests

Non-destructive inspection of samples with kissing bonding defect was made by using the ultrasonic Phased Array Pulse-Echo (PAPE) and ultrasonic Through Transmission Phased Array (TTPA) techniques. The PAPE method is appropriate for hybrid structures, because of cross-section picturing. Such analysis enables the observation of the adhesive line and detection of damages located on it [25]. The second, one of the most sensitive methods used in FML were used for kissing bonding detection. The TTPA method is appropriate for identification the wave attenuation, which can be a criterion for assessing the structural changes, without affecting the signal by secondary and interlayer wave reflections [26].

In case of the PAPE methods the defectoscope Omniscan MXU-M (Olympus, Japan) were used, with 64 piezoelements transducer (5L64 type of phased array head, Olympus Japan). The frequency 5 MHz, elevation 10.0 mm, active aperture 38.4 mm, pitch 0.6 mm were used. The TTPA analyses were made using the OmniScan MXII ultrasonic defectoscope (Olympus, Japan) and TomoView Inspection software for results analysis (Olympus, Japan). The TTPA tests also utilised the Olympus 5L64-I1 ultrasonic transducer (64 piezoelements, frequency 5 MHz, elevation 10.0 mm, active aperture 38.4 mm, pitch 0.6 mm), virtual aperture VPA (8 piezoelements, wave angle: 0°), and Olympus 5L64-I1 receiver transducer (64 piezoelements, frequency 5 MHz, elevation 10.0 mm, active aperture 38.4 mm, pitch 0.6 mm), virtual aperture VPA (8 piezoelements, wave angle: 0°). It was demonstrated through deep analysis, that the above parameters are effective in FML structures evaluation [25,26]. The test schemes were presented in Fig. 2.

The cross-section analysis of FML structure in the area with the kissing bonding in the cross-section plane is presented in Fig. 3.

As it was demonstrated in Fig. 3, the solution to simulation of a kissing bonding defect is effective. There is no visible delamination at the metal/composite interface. Simultaneously, the touching of metal and carbon/epoxy layer is real. The microstructure prepared in the place of the kissing bonding was applied, shows the normal structure of fibre metal laminates. The elements that belong to it are aluminium, anodising surface (oxide layer (Al2O3) [46], grey area between Al and epoxy matrix of composite, see. Fig. 3) and composite (carbon/epoxy) (see. Fig. 3). The significant observation is invisibility of Frekote layer at the metal/composite interface as a separate layer. There are two major reasons for the above phenomena. First is the spongy morphology of the oxide layer. The applied anodising based

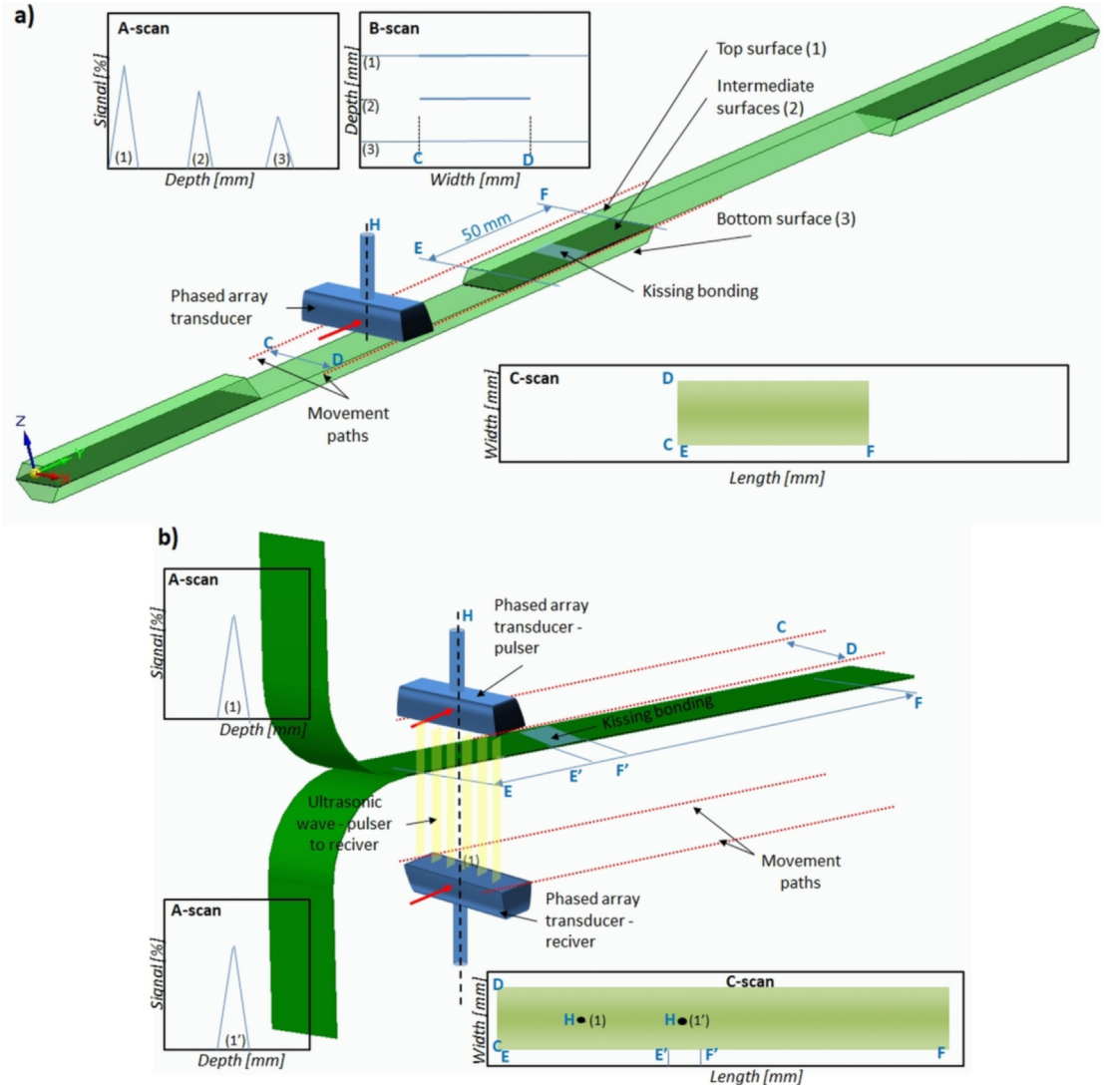

Fig. 2. Phased Array pulse-echo ultrasonic test on the example of SLS (a) and Phased Array through-transmission ultrasonic test on the example of T-peel (b).

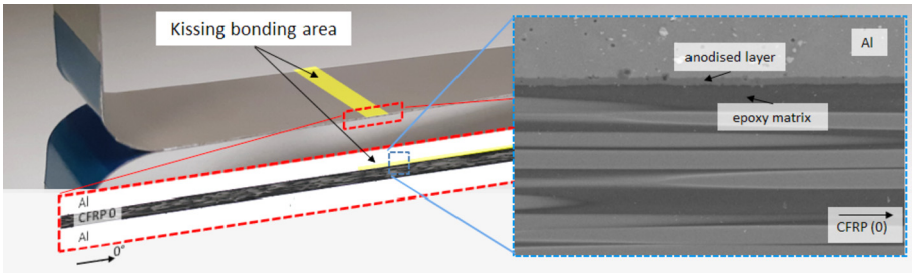

Fig. 3. The microstructure of FML and area with release agent.

on chromic acid anodizing (CAA, manufactured based on the aerospace standard in PZL Świdnik, a Leonardo Helicopters Company, Poland) generate on the aluminum surface firstly porous sub-layer and growing from its oxides with columnar nature [45,46]. The liquid phase of the Teflon film applied on such surface makes its soaking into the spongy oxide layer. In normal features, the epoxy matrix of composite, during the curing process, should flow into the empty spaces in the oxide layer. In the case of appropriate integration of epoxy matrix of composite and oxide layer, the properties of the metal/composite in FMLs shows a better fracture toughness than epoxy [43]. The second reason is related to the contamination process of an epoxy matrix and Teflon film. During the curing process, and the stage of partial transformation of the matrix into a liquid state, Teflon film can be integrated with the epoxy [31]. That is why the clear boundary of the Teflon and epoxy is invisible. The above fact is the reason, why kissing bonding is named “zero thickness delamination” in the worldwide literature [30–32]. All the above elements ensure that the Frecote (PTFE -based release agent, as kissing bonding defect)

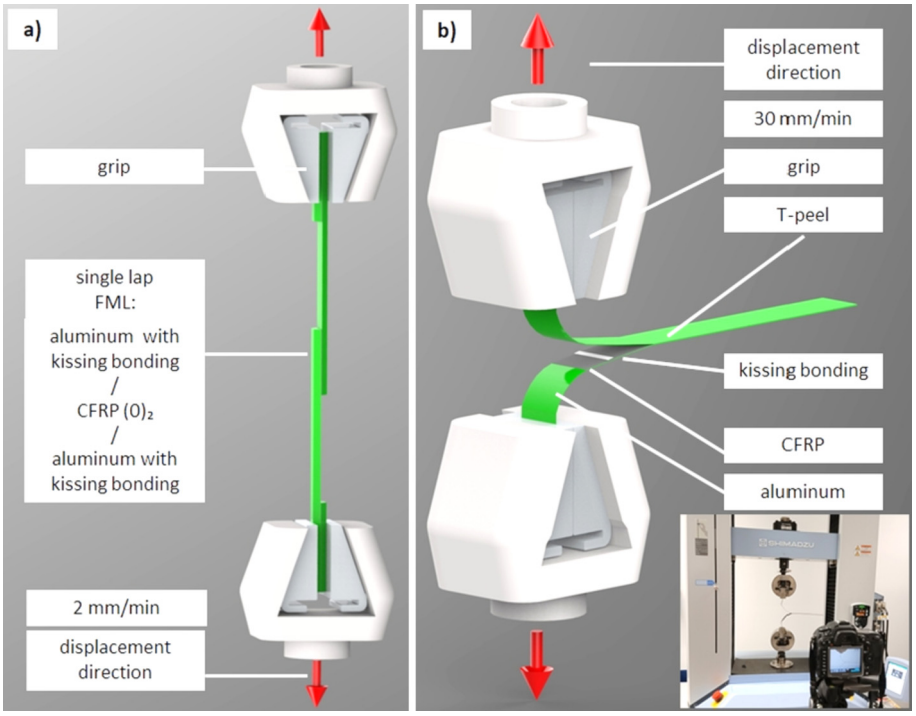

Fig. 4. The scheme of SLS (a) and T-peel (b) tests.

is an excellent representative of kissing bonding defects [30,35,36], which is also realistic for the industrial processes in composite manufacturing.

2.3. Strength tests

Two types of strength test were performed. The first one, single lap shear (SLS) test, was considered for the assessment of the kissing defect impact on in-plane load condition. The second one, T-peel test, was considered for the assessment of the kissing defect influence to out-of-plane load condition.

SLS test methodology was based on the ASTM D1002-01 [38]. To provide the possibility of manufacturing the appropriate share of the area of kissing bonding in total metal/composite adhesion area, the dimensions of the samples were enlarged in comparison to proposed by a ASTM D1002-01 standard [38] (Fig. 1). According to the designed dimensions (Fig. 1 and Table 1) the share of kissing bonding in SLS was 10%, 20%, 30% and 40% of total metal/composite adhesion area (1000 m^2). The SLS tests were conducted with a tensile speed of 2 mm/min.

T-peel tests were conducted according to ASTM D1876-08 [39]. The T-peel tests were conducted with the tensile speed of 30 mm/min. The scheme of the test was presented in Fig. 4.

For both tests, the force–displacement curves and the cracked surface images resulting from the fractured samples were reported and analysed in Section 3.

3. Results and discussion

3.1. NDT inspection

The ultrasonic non-destructive analysis of the samples type SLS (SLS_20mm) and T-peel (TP_0_20mm) are presented from Figs. 5–8. The 20 mm width of kissing bonding was presented as a representative case, which is characterized by the highest probability of detection (the highest share of “frekote” in the adhesive area).

As it can be seen on the Phased Array pulse-echo tests results of manufactured kissing bonding structure, the no differences can be visible between defective and normal area. The view of the total area of the sample with kissing bonding is homogeneous (C-scan maps, Figs. 5 and 6). Outside the kissing bonding area the signal level on the A-scans is the same as over the defected area. The full transparency of kissing bonding area for UT is obvious. No signal variations were observed for relatively that samples (SLS type of samples) and for thin samples (T-peel type of samples, overall thickness 0.8 mm). Even doubled frekote films, did not affect the UT sensitivity and detection possibilities. However, the release agent is not a foreign object, empty spaces of delaminated areas in FMLs for which the Phased Array UT method is the most effective [25]. Due to the fact, that the liquid release agent (reason of kissing bonding defect) cannot be visible in the structure, and is integrated with the epoxy resin and is soak into the anodised layer, its physical nature is different in comparison to other types of defect met in the FML structures. In general, foreign objects (like not-removed rests of the foils from manufacturing stages) or delaminations (empty spaces between separated layers) are characterized by other physical properties in comparison to the intact FML system even with the kissing bonding defects. Due to differences in attenuation (foreign objects) and reflections (delaminations) of the ultrasonic wave during propagation through defected FML is possible to identify this defect. In the case of a kissing bonding defect, the contact between each layer is a fact. Also, no elements of the FML where the local variations of the acoustic impedance possible to pure detection.

The Through Transmission Phased Array (TTPA) test results of SLS and T-peel samples with kissing bonding 20 mm width are presented in Figs. 7 and 8 respectively.

The TTPA tests results are similar to PA results. Both did not detect any kissing bonding areas. The key to damage identification in UT methods is the attenuation level, and without significant differences, focused on the expected areas (damaged via a frekote) of the attenuation, the C-scan maps will stay homogenous (C-scan map, Fig. 8). Even if the reference signal amplitude is set on 80%, the rather structural influence on the wave attenuation is visible, but not a kissing bonding

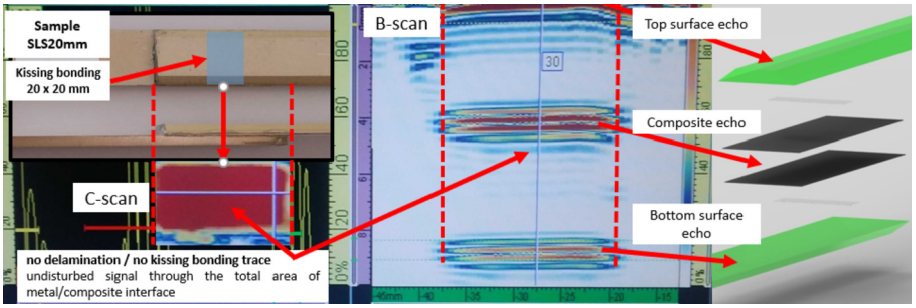

Fig. 5. Phased Array Pulse-echo test result of SLS sample with 20 mm width of kissing bonding.

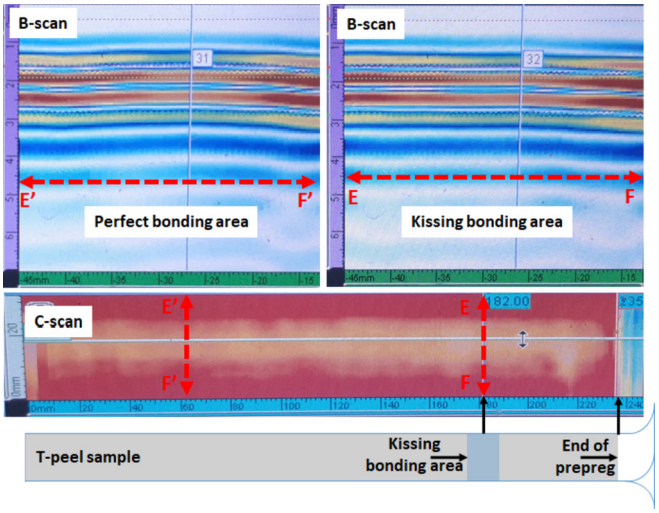

Fig. 6. Phased Array Pulse-echo test result of T-peel plate with 20 mm width of kissing bonding.

(C-scan maps, Fig. 7). The detailed analysis of signal attenuation was made using the coefficient signal-to-signal ratio. The use of the signal-to-signal ratio (SSR) index was delivered for the purpose of the kissing bonding identification (Eq. (1)).

$$SSR = \frac{f(x_k, y_p \in d_a)\_S_B}{f(x_n, y_m \notin d_a)\_S_A} \quad (1)$$

where:

$f(x_n,y_m \notin d_a)\_S_A$ is the value of the signal outside the kissing bonding area (signal B [%]) (see. Fig. 8)

$f(x_k,y_p \in d_a)\_S_B$ is the value of the signal in the kissing bonding area (signal A [%]) (see. Fig. 8)

d_a – area of simulated / defected area

x_n ; y_m ; x_k ; y_p - point coordinates in sample

SSR can be defined as the ratio of the maximum possible power of a signal outside the simulated defects to the power of a signal around the middle point of simulated defect (in case: kissing bonding). Using SSR gives the same boundary conditions for signal analysis in samples, even if specific noise is different for each sample. The place to a measure the signals in defined areas were random but with respect to the conditions: $x_n,y_m \notin d_a$ and $x_k,y_p \in d_a$. Two measured signals outside the kissing bonding area and two measured signals inside the kissing bonding area in each T-peel sample (examples of one signal from kissing bonding area and one from the area outside the kissing bonding were pointed on Fig. 8 – blue arrows) were calculated and presented in Table 3.

As it is applied in practice the 6 dB loss (or more) of wave signal is considered as a structural defect. This corresponds to a 50% decrease in the signal from the reference value (SSR value more about 0.5 or less). The physical kind of kissing bonding defect from the assumption will not have such drastic attenuation because of physical contact between individual layers. However, the detailed analysis of wave

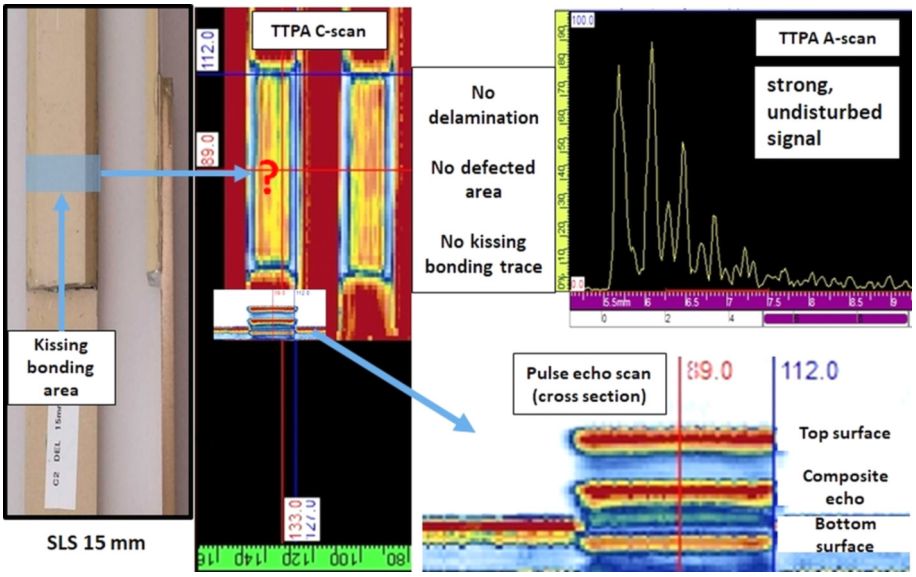

Fig. 7. Through Transmission Phased Array test result of SLS sample with 20 mm width of kissing bonding.

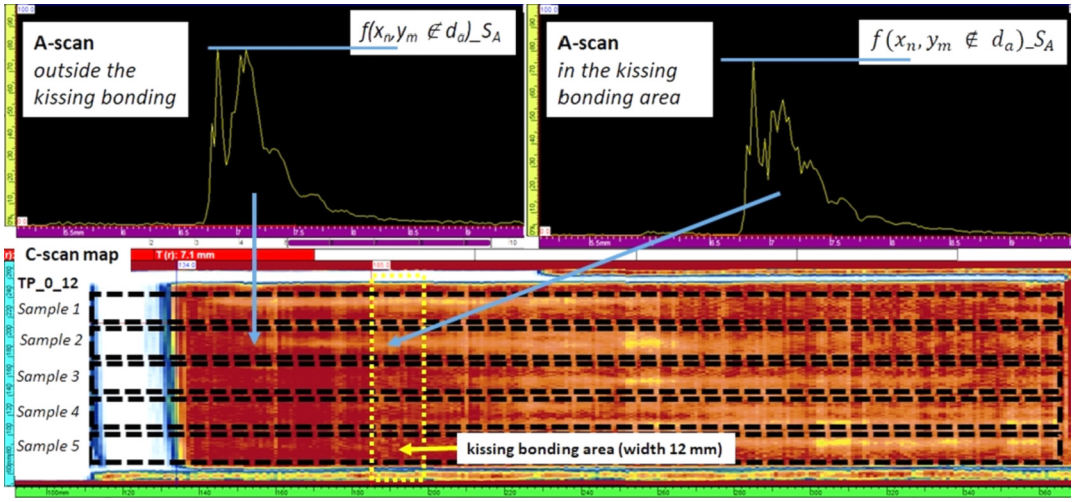

Fig. 8. Through Transmission Phased Array test result of T-peel plate with 20 mm width of kissing bonding.

Table 3
T-peel SSR analysis.

FML panel name	Sample no.				
	1	2	3	4	5
	SSR				
TP_0_4mm	0.93	1	1	1	0.99
TP_90_4mm	0.94	0.97	1.06	0.99	0.97
TP_0_12mm	0.9	0.96	1	0.93	0.96
TP_90_12mm	0.99	0.89	0.99	1.1	1.07
TP_0_20mm	0.98	1	1	0.92	0.99
TP_90_20mm	1.1	0.96	1	0.96	1.01

attenuation, presented in Table 3, cannot show any pattern and repetitive of wave attenuation due to kissing bonding area. The measurements were conducted straightly over the kissing bonding area for each tested sample and in the place near the kissing bonding defect. The maximum difference of attenuation between area over the kissing bonding and normal adhesion is 11% (case TP_90_12mm). Even if some SSR variations can be observed in Table 3, there are not caused by a kissing bonding area, but by composite features (variations in local fibre and matrix content). This phenomenon is confirmed by cases were SSR parameter is higher than 1, which indicate that the attenuation in the perfect bonding area was higher than in the kissing bonding area (even a 10% higher – e.g. case TP_90_20mm, Table 3). Summarizing, based on NDT results, with highly sensitive methods, the kissing bonding defect in FMLs is not detectable because of the strong adjacency of individual layers in FML. This is because of not only physical contact between layers but also the liquid nature of kissing bonding defects (relies films, oil, etc.). The acoustic impedance of this type of media, and the thickness equal near-zero (liquid media fill the unevenness of the aluminium surface) causes practical transparency for ultrasonic wave. Moreover, the above facts are the same barrier for other types of NDT methods, such as thermography, eddy-currents, tomography etc.

Possible is that the kissing bonding is the area with a weak adhesion (not without any adhesive strength), which means that the layers touching is characterized by kind of adhesion and surfaces compressibility and matching. The strength aspect will be presented in the next sections.

3.2. In-plane shear strength of metal/composite interface

The force – displacement and mean values of maximum force of SLS samples were presented in Fig. 9.

The first stage of increasing force is quite linear until 0.4 mm of displacement for all the tested case (Fig. 9). After this two characteristic FMLs responses were noted. The first is the stiffness reduction and further force increasing as in the case of sample SLS ref no. 1, samples SLS 5 mm no. 1 and 2 and samples SLS 15 mm no. 2 and 3. The second one is a rapid drop of force at about 500–1000 N per 0.01–0.02 mm of displacement and further force increasing. Both observed phenomena are related to crack formation. However, the stiffness reduction is caused by initiation and propagation correlated with the displacement, in contrast to the second phenomena where higher stress accumulation and rapid crack propagation can be expected. Based on the results of in-plane shear strength can be stated generally, that kissing bonding causes a reduction of in-plane shear strength of FML. However, despite the four times larger area of kissing bonding (from 100 mm^2 – sample SLS_5 mm until 400 mm^2 – sample SLS_20 mm) the strength reduction equal ~ 19% (mean values, Fig. 9). Based on this, it can be expected, that the kissing bonding does have some strength, and the force applied to first breaking up this bonding is needed [30]. Two major factors can justify this. The first one is that the kissing bonding have marginal strength, and the force applied to prior break-up of the bonding is needed (it was also presented in the out-of-plane t-peel test). In practice, at the beginning process of the load, the displacement is low, and the most important is the initial in-plane strength [correlated with the ref. 39,49]. Increasing the displacement causes the initiation process of the delamination due to shear stresses increase. And then the rapid crack at kissing bonding occurs what reduces the real adhesion area which also means that the overall strength is limited. The second one is related to the shear stress growth in the SLS sample configuration. As it was presented in detail by Kumar et al. [30], Her [47] and He [48], stress concentration is higher at the edges of an adhesive joint due to geometrical discontinuity leading to strain localization in the region. It shows, that the central located kissing bonding area has a limited impact on the initial behavior on a load of the single-lap joints. The fractured surface of SLS samples (reference and with various area of kissing bonding) are presented in Fig. 10.

As it can be observed on fractured surfaces of SLS samples the dominant failure has a cohesive nature. The reference sample is damaged with a cohesive type of failure. The fracture of SLS_ref type of FMLs was initiate by a interlaminar share at the metal/composite interface near the edge (Fig. 10 a). But finally shear fracture was transferred to composite (0)/composite (0) interface - the poorest element of the SLS FML configuration. Above can be an additional factor of not significant reduction of shear strength despite the increasing share of kissing bonding area. As the share of the kissing bonding increases the failure type becomes mixed – cohesive/adhesive. However, the locations of

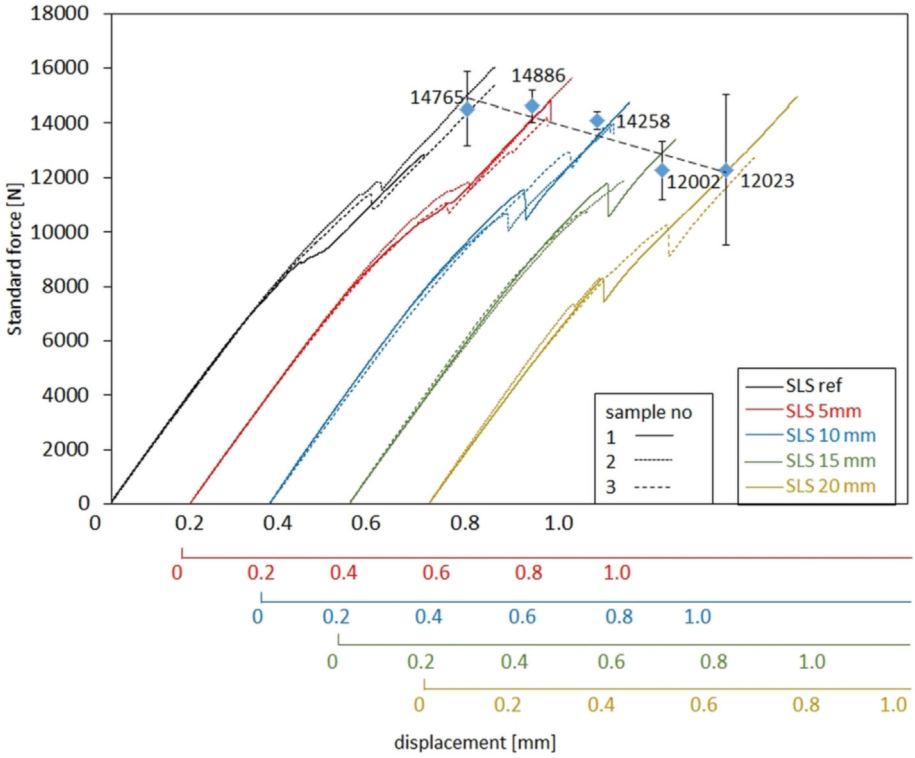

Fig. 9. SLS results for FMLs with different kissing bonding widths.

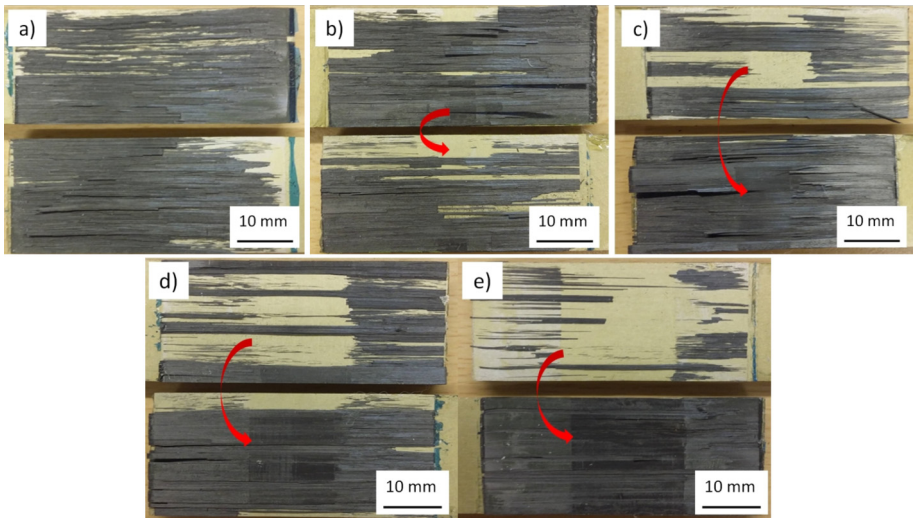

Fig. 10. The fracture surface after SLS test of reference FMLs (a) and FMLs with kissing bonding width 5 mm (b), 10 mm (c), 15 mm (d) and 20 mm (e).

the adhesive type of failure are not random. It can be observed, that the adhesive type of failure is precisely correlated with the kissing bonding area (Fig. 10). The fact of local changes of the failure type is caused by poor adhesion (frekote area) and contamination phenomena of composite with release agent (dark areas visible on composite layer, Fig. 10) [31]. Because of two not poor matching behaviours of FMLs with kissing bonding after in-plane shear load (not significant strength reduction and evident impact of kissing bonding to failure formation), the more critical type of load was proposed - t-peel test.

3.3. Fracture properties of metal/composite interface

The representative force–displacement curves of FMLs (0) and (90) with kissing bonding defects after t-peel test were presented in Figs. 11 and 12 respectively.

The force–displacement curves after t-peel test of FMLs are characterized by the beginning peak of force which is the point of the initial crack threshold and further descending of force. The smooth nature of force descending is characterized more to FML (0) than FML (90)

(Figs. 11 and 12 respectively) because of less share of transverse matrix cracking when the fibres are along the peel direction. Nonetheless, independent on fibre direction, the FML with the proper adhesive at the metal/composite interface (due to surface preparation) is characterized by a cohesive type of fracture in the composite after the peel test. The differences in the character of force - crack growth between FML(0) (Fig. 11) and FML (90) (Fig. 12) can be explained by a cleavage stress theory (see. Eq. (2)) [40].

$$\sigma = \sigma_0(cos\beta d + Ksin\beta d)e^{\beta d} \tag{2}$$

where:

$$\beta = \left(\frac{Yw}{4EIa}\right)^{1/4} \tag{3}$$

and

$$K = \frac{\beta m}{\beta m + sin\theta} \tag{4}$$

where:

σ – cleavage stress at distance d of metal - composite adhesive [MPa]

σ_0 - boundary cleavage stress at x = 0 [MPa]

d – the distance along t-peel of adhesive [mm]

Y – Young modulus of adhesive [GPa]

E – Young modulus of adherend [GPa]

a – adhesive layer thickness [mm]

w – bond width [mm]

I – moment of inertia of the adherent cross-section [mm4]

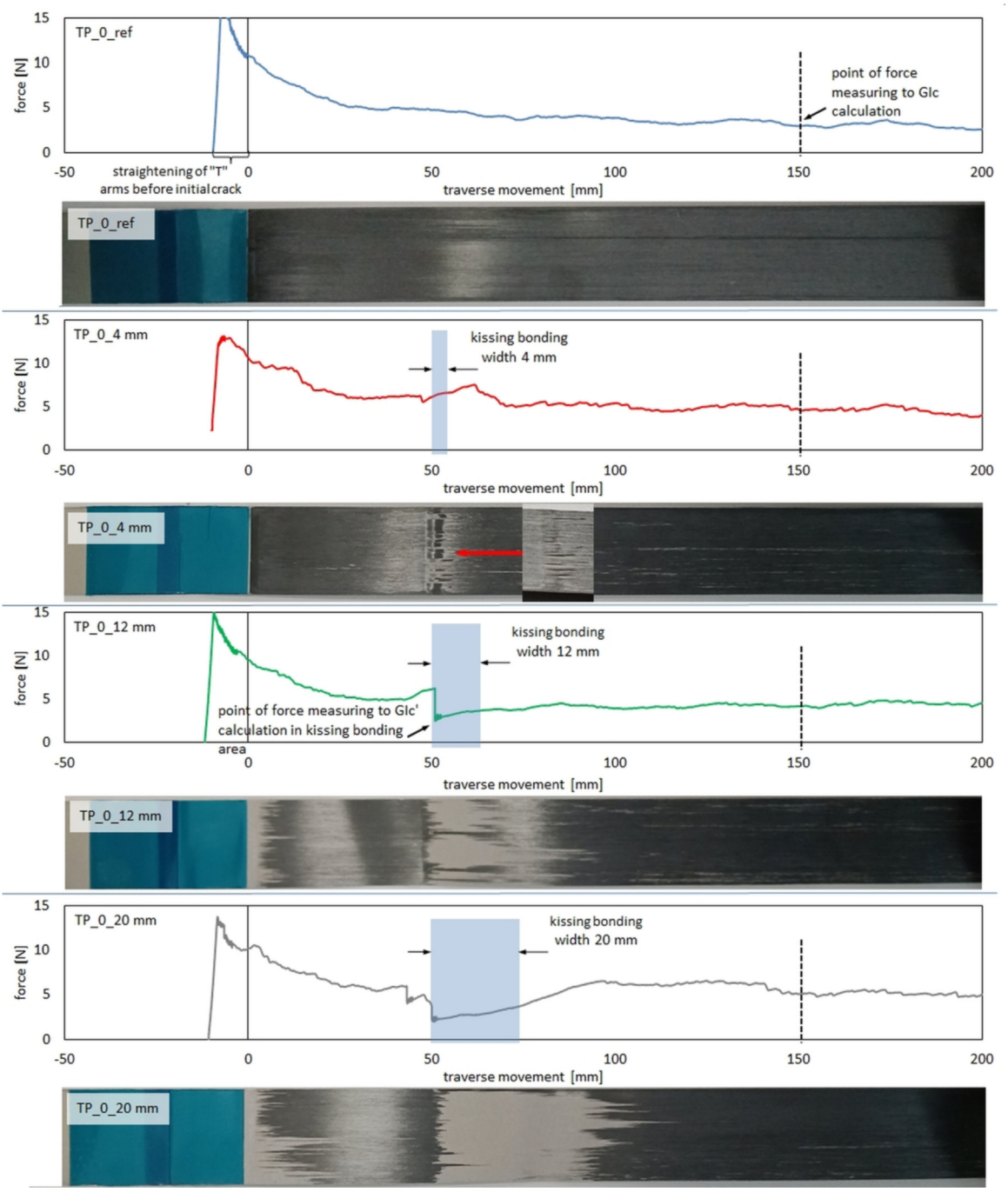

Fig. 11. The force–displacement curves of FMLs (0°) with various kissing bonding width.

m – moment arm of peel force [mm]

θ – peel angle

According to Eqs. (2) and (3) the cleavage stress at a random distance along t-peel of adhesive is dependent on some materials and geometrical factors. In the case of t-peel of appropriate metal-composite adhesive, the higher meaning has material factors. The major feature which changes when the t-peel of FML(0) and FML (90) occurs is the Young modulus of an adherent. Due to crack propagation inside the composite (considered in FML as an adhesive component), the stiff carbon fibres interact with the adherent (aluminium). The fibre orientation along with the sample length cause quite constant stiffness of adherent and quasi-linear crack growth (and force path) in the adhesive area. The different situation is in the case of FML (90). The perpendicular fibre orientation cause crack migration between fibres, which means that the local stiffness of an adherent is change as well as the crack direction not always longitudinal orientated to the adhesive plane. In result, force fluctuations can be observed. The sudden drop of force and simultaneous change of damaged interlayer in

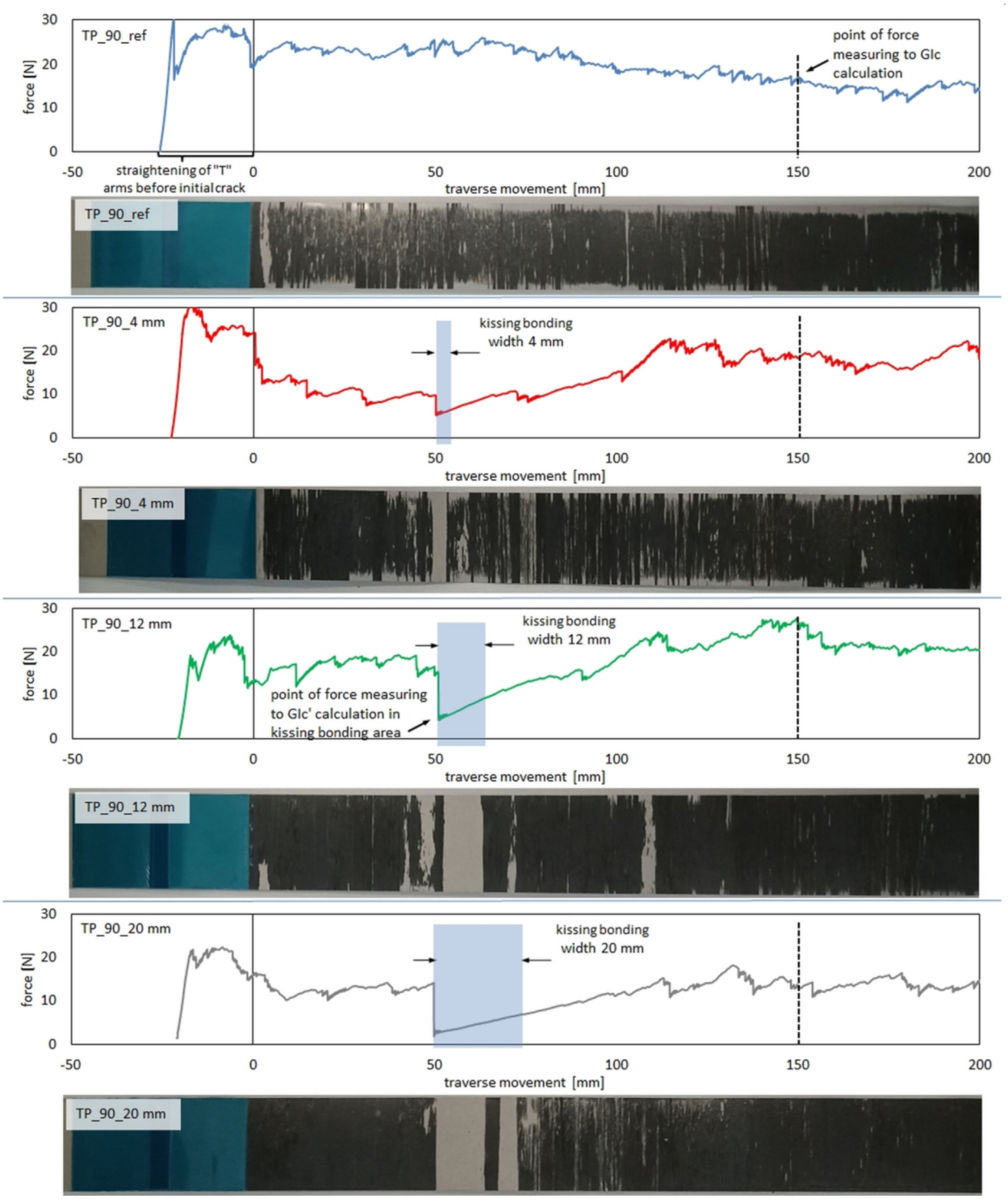

Fig. 12. The force–displacement curves of FMLs (90°) with various kissing bonding width.

FML was observed over the total area of kissing bonding, independent on fibre architecture (Figs. 11 and 12). The force behaviour can be also explained by stress theory when the kissing bonding area is considered. Because of lack of adhesion at the metal - composite in the kissing bonding area the material features of adherent and adhesive are the same for both type of FMLs. However, rapid crack opening at the metal - composite in the kissing bonding area occurs, the peel angle and moment arm of peel force are changing (spring response of aluminum arm). Simultaneously, stress relaxation occurs. The force drops significantly. However, constant sample opening occurs and force level is slowly back to previous levels (Figs. 11 and 12). The spring effect of the aluminium arm due to lack of adhesion area can be proved by a changing the angle ($\Delta\Omega = \Omega_2/\Omega_1$) between both peeled arms before kissing bonding (Ω_1), over the kissing bonding area (Ω_2). The visualization of the Ω angle is presented in Fig. 13. The Ω angle equal 2θ (when he gravity effect is neglected [42,44]).

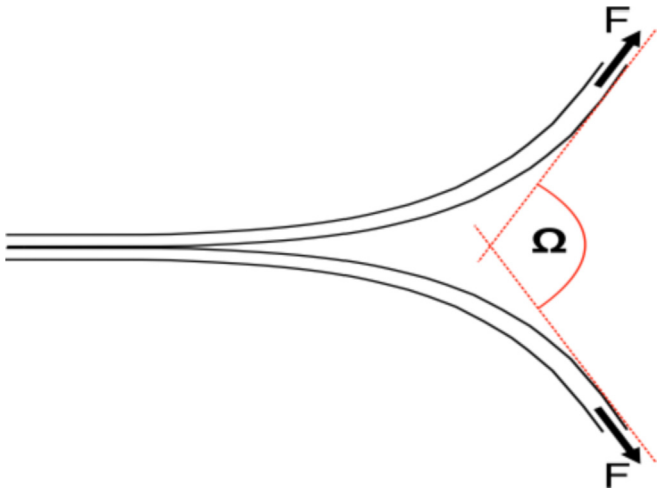

Fig. 13. The scheme of the angle (Ω) between both peeled arms.

Table 4
The values of the ΔΩ different kissing bonding variants.

FML sample	Ω_1 [rad]	Ω_2 [rad]	ΔΩ
TP_0_ref	1.61 (±0.01)	–	–
TP_0_4mm	1.62 (±0.05)	1.57 (±0.06)	0.97
TP_0_12mm	1.54 (±0.05)	1.42 (±0.05)	0.92
TP_0_20mm	1.42 (±0.07)	1.30 (±0.03)	0.92
TP_90_ref	2.15 (±0.03)	–	–
TP_90_4mm	1.97 (±0.02)	1.88 (±0.05)	0.95
TP_90_12mm	2.44 (±0.09)	2.27 (±0.08)	0.93
TP_90_20mm	2.13 (±0.06)	1.94 (±0.05)	0.91

The values of the angle were presented in Table 4.

The analysis of the ΔΩ shows that the kissing bonding area has an impact on the stress relaxation of the peeled FMLs arms. The lack of adhesion leads to faster energy release. Significant differences can be observed between FML with various fibre orientation. The FML (0) can be characterized by a relatively low peel angle in comparison to FML (90). The simple explanation concern the stiffness of the arm. As it was presented in Fig. 11, in the case of FML (0) the crack propagate as a translaminar fracture of carbon composite. It causes the higher stiffness of a peeled arm due to its hybrid nature (aluminum - longitudinal carbon fibres). In the case of FML (90) the perpendicular carbon fibres do not cause a significant increase in arm stiffness. Is also visible, that the lack of adhesion width has an impact on stress relaxation of peeled arms. When the width increase, the peel angle become lower due to the higher distance of arms free straightening.

Simultaneously with the arm spring effect, the fracture mechanisms are changing. The wider the kissing bonding area the clearer the impact on fracture can be seen. Even in the case of FML_0_4mm sample, the de-adhesion of fibres at the metal-composite interface is visible, despite the keeping intact of fibres (Fig. 11). This effect results from enough strength of carbon fibres to transverse force as a result of local changing the degradation plane in FML (from composite-composite to composite-metal and reverse). By the assumptions of quasi-static (no kinetic energy) and steady-state conditions (elastic energy stored in the strips is only due to bending and constant due to inextensibility assumptions) [41] the rate of total external work (W) can be expressed by Eq. (5).

$$W = 2P * v = (\gamma + \delta) * b * v \tag{5}$$

where:

γ and δ denote the debonding and dissipative energies, respectively, per unit area of crack advance

b – sample width [mm]

v - velocity (m/s) of point of application of peel forces

P – force [N]

In particular, if δ is zero, and symmetrical loading and material properties prevail on both sides of the interface such that the failure of the interface occurs purely by opening mode, then γ represents the mode I fracture toughness (G_{Ic}) of the interface [41,42]. The δ was estimated as zero value, because of measured forces (less than 30 N) and cross-section of one strip (6 mm^2) means that the possible stress value in the strip is less than 5 MPa, which is much under the elastic limit for Al-2024 T3. Those means that Eq. (5) can be simplified to Eq. (6), and it is appropriate to the comparison of the kissing bonding zone and areas with normal adhesion.

$$\gamma = \frac{2P}{b} = G_{Ic} \tag{6}$$

where:

G_{Ic} – adhesive fracture energy in mode I [N/mm]

Table 5
The peeling parameters for normal adhesion and kissing bonding in FMLs.

FML sample	$N/mm_{(150)}$	$N/mm'_{(kb)}$	G_{Ic}	G_{Ic}'
TP_0_ref	0.164 *(±0.03)*	–	0.329 *(±0.05)*	–
TP_0_4mm	0.189 *(±0.01)*	0.187 *(±0.02)*	0.377 *(±0.02)*	0.374 *(±0.04)*
TP_0_12mm	0.192 *(±0.02)*	0.145 *(±0.03)*	0.385 *(±0.03)*	0.290 *(±0.07)*
TP_0_20mm	0.258 *(±0.03)*	0.09 *(±0.02)*	0.516 *(±0.16)*	0.194 *(±0.03)*
TP_0 average	**0.2**	**0.14 *(↓−30%)***	**0.40**	**0.29 *(↓−27.5%)***
TP_90_ref	0.830 *(±0.12)*	–	1.660 *(±0.24)*	–
TP_90_4mm	0.795 *(±0.13)*	0.300 *(±0.09)*	1.589 *(±0.27)*	0.600 *(±0.19)*
TP_90_12mm	0.819 *(±0.08)*	0.173 *(±0.02)*	1.639 *(±0.16)*	0.345 *(±0.04)*
TP_90_20mm	0.636 *(±0.08)*	0.077 *(±0.01)*	1.272 *(±0.16)*	0.154 *(±0.02)*
TP_90 average	**0.77**	**0.18 *(↓−76.6%)***	**1.54**	**0.37 *(↓−75.9%)***

The values of peel force per unit width (measured in the distance 150 mm of peeling - **N/mm$_{(150)}$** and in the kissing bonding down-peak force - **N/mm'$_{(kb)}$**) as well as **G$_{Ic}$** and **G$_{Ic}$'** (apostrophe indicates the value for the kissing bonding) were presented in Table 5.

The results of a study on the interlaminar fracture toughness properties (critical adhesive fracture energy which represents mode I fracture toughness (G_Ic) of the interface) in all samples resulted from composite de-cohesion. It can be noted that the average interlaminar

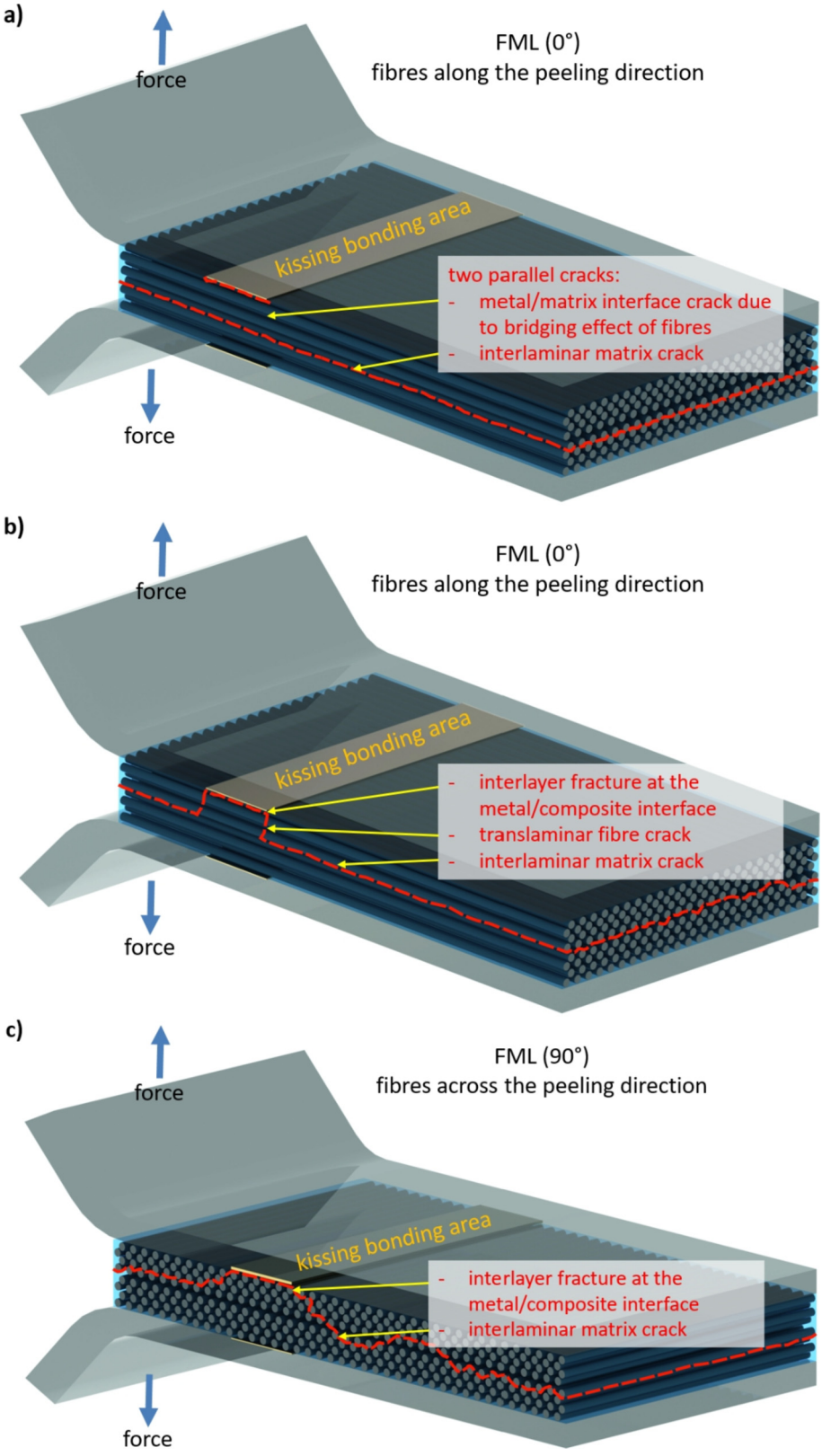

Fig. 14. The mechanisms of crack propagation in contact with the kissing bonding defects in FML dependent on fibre direction: along with peeling (a,b) and perpendicular (c).

fracture toughness of FML outside the kissing bonding area is nearly four times larger (0.4 to 1.54 N/mm, see Table 4) for FMLs with perpendicular fibre orientation in order to t-peel direction. The presence of fibres with an orientation other than 0° reduces the value of G_Ic parameter in FMLs [42]. This fact is connected with the stiffness of a strip during the peel-test. The strip is stiffer if the fibres (0) are integrated with it. This results in a tendency to straightening of a strip during peel test, and easier opening the FML in the composite layer. The results of a study on the interlaminar fracture toughness properties over the kissing bonding area (distorted mode I fracture toughness of the interface - G_{Ic}') show that the release agent on the aluminium surface has a significant impact on the adhesive properties at the metal-composite interface in FMLs. In the case of FML (0) the reduction was almost 30% (average), while for FML (90) exceeded 75% (average). Moreover, the tendency of increasing the reduction scale was obvious with the increasing of the kissing bonding width (Table 5).

Based on the observations of damage of fractured area after t-peel tests, as well the analysis of calculated values, two types of crack formation mechanisms due to kissing bonding can be described in a model way (Fig. 14).

In the case of FMLs with the perpendicular fibre orientation to the peel direction the one failure pattern occurs. This is an interlayer fracture through the epoxy matrix in FML section with appropriate bonding, and crack migration to the metal/composite interface in the poor adhesion. The above is due to kissing bonding defect and immediately behind the kissing bonding area starting a new crack migration to composite matrix volume (Fig. 14c). In the case of FMLs with the direction of the longitudinal fibres to peel direction two failure pattern occurs. Depending on the poor adhesion area width the interlayer fracture in the composite can be observed until kissing bonding defect area and then transfer the crack to the metal/composite interface through fibres (translaminar fibre crack, see Fig. 14b). In the case of low width of poor adhesion area, the two parallel interlaminar cracking can be seen, one at the metal/composite interface in poor adhesion area, the second continuous in the composite layer (Fig. 14a). The translaminar fibre crack type of fracture can cause more significant loss of local peel force and reduction of strain energy release rate in mode I, while the two parallel interlaminar cracking type of failure, due to constant major path of matrix cracking, can cause an only small variation of peel strength.

4. Summarizing

4.1. Background

The purpose of the work was the evaluation of kissing bonding defects in fibre metal laminates by using NDT techniques appropriate for FMLs and the impact of this type of defect to in-plane and out-of-plane mechanical properties. As it was described, the FMLs are the materials with numerous interfaces with different physical properties, which is problematic for lack adhesion area recognition. Simultaneously, the perfect adhesion at the interfaces is critical for fatigue or post-impact properties.

4.2. Detection

The ultrasonic phased array pulse-echo and through transmission phased array were selected as NDT methods. It was presented that even sensitive UT methods are not able to detect the kissing bonding defect in FML. This is because of not only physical contact between layers but also the liquid nature of kissing bonding defects (relies films, oil, etc.). The acoustic impedance of this type of media, and the thickness equal near-zero (liquid media fill the unevenness of the aluminium surface) cause practical transparency for ultrasonic wave.

4.3. Impact on mechanical properties and fracture

For the assessment of the impact of the kissing bonding defects on properties on FML the in-plane shear and out-of-plane peel test was conducted. Based on the mechanical test was presented that the type of failure is correlated with the kissing bonding area. However, in the case of in-plane shear strength, not significant strength reduction was observed for kissing bonds with different widths. This suggesting that the kissing bonding does have some initial strength and the force to first breaking up is needed. In case of t-peel test was observed that release agent on the aluminium surface has a significant impact on the adhesive properties at the metal-composite interface in FMLs. In the case of FML (0) the reduction was almost 30%, while for FML (90) exceeded 75%. Moreover, the tendency of increasing the reduction scale was obvious with the increasing of the kissing bonding width. The reason for poor mechanical properties of the metal/composite interface in the defective surface by the kissing bonding is the no effective adhesion between the epoxy matrix of the composite component of FML and the anodised surface of aluminum. The PTFE-based liquid release agent, used as a kissing bonding defect, soaks the porous and columnar Al2O3 sub-layer build in the chromic acid anodising process of aluminium. Additionally, the contamination effect of the release agent and epoxy during the curing process occurs. In fact, such an area can be characterized by non-separated volume in the FML structure and simultaneously does not keep the appropriate properties because due to lack of interaction n between the epoxy and anodised layer. The lack of adhesion is the result of changing the crack paths propagation during mode I of FML. Finally, two types of crack formation mechanisms due to kissing bonding were described. It was observed that some damage mechanisms are possible for specific FML construction: (1) parallel cracking of matrix cracks and metal/composite interface, (2) one interlaminar crack with migration to the metal/composite interface or (3) crack propagation through various interlayers with fibre cracking in poor adhesion area.

4.4. Future works

The problems with the detection of kissing bonding defects are the base of findings in other types of NDT techniques. The possibilities of vibration-based methods will be considered. Moreover, based on current work, the kissing bonding defects impact during more complex stresses-state will be investigated, such as impact (out-of-plane) or fatigue (in-plane).

Declaration of Competing Interest

The authors declare that they have no known competing financial interests or personal relationships that could have appeared to influence the work reported in this paper.

Acknowledgments

The research was conducted partially at Delft University of Technology based on long-term cooperation, for which authors are grateful.

The project/research was financed in the framework of the project Lublin University of Technology-Regional Excellence Initiative, funded by the Polish Ministry of Science and Higher Education (contract no. 030/RID/2018/19).

Data availability

Data available on request from the authors.

References

[1] Vlot A, Gunnink JW. Fiber metal laminates – an introduction. Dordrecht, The Netherlands): Kluwer Academic Publishers; 2001.
[2] Sinmazçelik T, Avcu E, Bora MO, Çoban O. A review: Fibre metal laminates, background, bonding types and applied test methods. Mater Design 2011;32(7):3671–85.
[3] Ostapiuk M, Surowska B, Bieniaś J. Interface analysis of fiber metal laminates. Compos Interface 2014;21(4):309–18.
[4] Wu X, Zhan L, Zhao X, Wang X, Chang T. Effects of surface pre-treatment and adhesive quantity on interface characteristics of fiber metal laminates. Compos Interfaces 2020;27(9):829–43.
[5] Alderliesten RC. Analytical prediction model for fatigue crack propagation and delamination growth in Glare. Int J Fatigue 2007;29(4):628–46.
[6] Dadej K, Bieniaś J, Surowska B. Residual fatigue life of carbon fibre aluminium laminates. Int J Fatigue 2017;100(1):94–104.
[7] Surowska B, Ostapiuk M, Jakubczak P, Droździel M. The durability of an organic-inorganic sol-gel interlayer in Al-GFRP-CFRP laminates in a saline environment. Materials 2019;12(15):2363.
[8] Peng Z, Nie X. Galvanic corrosion property of contacts between carbon fiber cloth materials and typical metal alloys in an aggressive environment. Surf Coat Technol 2013;215:85–9.
[9] Cai BP, Liu YH, Ren CK, Liu ZK, Tian XJ, Abulimiti ABB. Experimental study of galvanic corrosion behaviour of carbon fibre composite coupled to aluminium in artificial seawater. Corros Eng Sci Technol 2012;47(4):289–96.
[10] Jakubczak P, Bieniaś J, Droździel M. The collation of impact behaviour of titanium/carbon, aluminum/carbon and conventional carbon fibres laminates. Thin Walled Struct 2020;155:106952.
[11] Sadighi M, Alderliesten RC, Benedictus R. Impact resistance of fibre-metal laminates: a review. Int J Impact Eng 2012;49:77–90.
[12] Jakubczak P, Bieniaś J, Droździel M, Podolak P, Harmsza A. The effect of layer thicknesses in hybrid titanium - Carbon Laminates on Low - Velocity Impact Response. Materials 2020;1(13):1–17.
[13] Dhaliwal GS, Newaz GM. Compression after impact characteristics of carbon fiber reinforced aluminum laminates. Compos Struct 2017;160:1212–24.
[14] Kumar DS, Asokan R. Compressive strength of the GLARE composite laminates after impact load. IJISET 2015;2(3):313–8.
[15] Düring D, Petersen E, Stefaniak D, Hühne C. Damage resistance and low-velocity impact behaviour of hybrid composite laminates with multiple thin steel and elastomer layers. Compos Struct 2020;238:111851. https://doi.org/10.1016/j.compstruct.2019.111851.
[16] Dadej K, Valvo P, Bieniaś J. The effect of transverse shear in symmetric and asymmetric end notch flexure tests-analytical and numerical modeling. Metals 2020;13(14):3046.
[17] Lawcock G, Ye L, Mai YW, Sun CT. The effect of adhesive bonding between aluminum and composite prepreg on the mechanical response of carbon-fiber-reinforced metal laminates. Compos Sci Technol 1997;57:35–45.
[18] Chai GB, Manikandan P. Low velocity impact response of fibre-metal laminates- a review. Compos Struct 2014;107:363–81.
[19] Mazaheri F, Hosseini-Toudeshky H. Low-cycle fatigue delamination initiation and propagation in fibre metal laminates. Fatigue Fract Eng M 2015;38(6):641–60.
[20] Bieniaś J, Dadej K. Fatigue delamination growth of carbon and glass reinforced fiber metal laminates in fracture mode II. Int J Fatigue 2020;130:1–11.
[21] Abouhamzeh M, Nardi D, Leonard R, Sinke J. Effect of prepreg gaps and overlaps on mechanical properties of fibre metal laminates. Compos Part A 2018;114:258–68.
[22] Croft K, Lessard L, Pasini D, Hojjati M, Chen J, Yousefpour A. Experimental study of the effect of automated fiber placement induced defects on performance of composite laminates. Compos Part A Appl Sci Manuf 2011;42(5):484–91.
[23] Lan M, Cartié D, Davies P, Baley C. Microstructure and tensile properties of carbon-epoxy laminates produced by automated fibre placement: influence of a caul plate on the effects of gap and overlap embedded defects. Compos Part A Appl Sci Manuf 2015;78:124–34.
[24] Nardi D, Abouhamzeh M, Leonard R, Sinke J. Detection and evaluation of pre-preg gaps and overlaps in glare laminates. Appl Compos Mater 2018;25:1491–507.
[25] Jakubczak P, Nardi D, Bieniaś J, Sinke J. Non-destructive testing investigation of gaps in thin Glare laminates. Nondestruct Test Eva 2021;36(1):17–34. https://doi.org/10.1080/10589759.2019.1684489.
[26] Jakubczak P, Bieniaś J. Non-destructive damage detection in fibre metal laminates. J Nondestruct Eval 2019;38(2):49.
[27] Meola C, Carlomagno GM, Squillace A, Vitiello A. Non-destructive evaluation of aerospace materials with lock-in thermography. Eng Fail Anal 2006;13:380–8.
[28] Sinke J. Some inspection methods for quality control and in-service inspection of GLARE. Appl Compos Mater 2003;10:277–91.
[29] Fahr A, Chapman CE, Laliberte JF, Forsyth DS, Poon C. Nondestructive evaluation methods for damage assessment in Fiber-Metal Laminates. Polym Compos 2000;21:568–75.
[30] Vijaya Kumar RL, Bhat MR, Murthy CRL. Evaluation of kissing bond in composite adhesive lap joints using digital image correlation: Preliminary studies. Int J Adhes Adhes 2013;42:60–8.
[31] Jeenjitkaew C, Luklinska Z, Guild F. Morphology and surface chemistry of kissing bonds in adhesive joints produced by surface contamination. Int J Adhes Adhes 2010;30:643–53.
[32] Nagy PB. Ultrasonic classification of imperfect interfaces. J Adhes Sci Technol 1991;5(8):619–30.
[33] Jiao D, Rose JL. An ultrasonic interface layer model for bond evaluation. J Adhes Sci Technol 1991;5(8):631–46.
[34] Markatos DN, Tserpes KI, Rau E, Markus S, Ehrhart B, Sp P. The effects of manufacturing-induced and in-service related bonding quality reduction on the mode-I fracture toughness of composite bonded joints for aeronautical use. Compos Part B 2013;45:556–64.
[35] Tighe RC, Dulieu-Barton JM, Quinn S. Identification of kissing defectsin adhesive bonds using infrared thermography. Int J Adhes Adhes 2016;64:168–78.
[36] Jeenjitkaew C, Guild FJ. The analysis of kissing bonds in adhesive joints. Int J Adhes Adhes 2017;75:101–7.
[37] Jakubczak P, Bieniaś J, Mania R, Majerski K. Forming of thin–walled profiles made of FML in autoclave process. Aircr Eng Aerosp Tec 2018;90(3):506–14.
[38] ASTM D1002-01 Standard Test Method for Apparent Shear Strength of Single-Lap-Joint Adhesively Bonded Metal Specimens by Tension Loading, 100 Barr Harbor Drive, West Conshohocken, PA 19428-2959, United States
[39] ASTM D1876-08 Standard Test Method for Peel Resistance of Adhesives (T-Peel Test), 100 Barr Harbor Drive, PO Box C700, West Conshohocken, PA 19428-2959. United States
[40] Kaelble DH. Theory and analysis of peel adhesion: bond stresses and distributions. Trans Soc Rheol 1960;4:45–73.
[41] Zarei H, Marulli MR, Paggi M, Pietrogrande R, Üffing C, Weißgraeber P. Adherend surface roughness effect on the mechanical response of silicone-based adhesive joints. Eng Fract Mech 2020;240:107353.
[42] Padhye N, Parks DM, Slocum AH, Trout BL. Enhancing the performance of the T-peel test for thin and flexible adhered laminates. Rev Sci Instrum 2016;87:085111.
[43] Bieniaś J, Dadej K, Surowska B. Interlaminar fracture toughness of glass and carbon reinforced multidirectional fiber metal laminates. Eng Fract Mech 2017;175:127–45.
[44] Gent AN, Lai S-M. Interfacial bonding, energy dissipation, and adhesion. J Polym Sci Part B: Polym Phys 1994;32:1543.
[45] Venables JD. Review adhesion and durability of metal-polymer bonds. J Mat Sci 1984;19(8):2431–53.
[46] Patermarakis G, Moussoutzanis K. Electrochemical kinetic study on the growth of porous anodic oxide films on aluminium. Electrochemica Acta 1995;40(6):699–708.
[47] Her S-C. Stress analysis of adhesively-bonded lap joints. Comp Struct 1999;47(1-4):673–8.
[48] He X. A review of finite element analysis of adhesively bonded joints. Int J Adhes Adhes 2011;31(4):248–64.